Modified Lennard-Jones potentials for Cu and Ag based on the dense gaslike model of viscosity for liquid metals

Y. N. Zhang, L. Wang,* S. Morioka, and W. M. Wang
Key Laboratory of Liquid Structure and Heredity of Materials, Ministry of Education, Shandong University, Jinan, 250061, People's Republic of China

(Received 2 July 2006; revised manuscript received 18 October 2006; published 10 January 2007)

Based on the dense gaslike model of viscosity, we have obtained the modified Lennard-Jones potentials suitable for studying the liquid structure of Cu and Ag. Experimental data considered in deriving the potentials include the liquid density, viscosity, and pair correlation function. The energy and structural properties of liquid Cu and Ag in cooling processes have been studied via molecular dynamics simulations, exhibiting correct trends as a function of temperature. Calculated results are comparable with those derived by Johnson's embedded-atom method (EAM) and effective pair potential. The differences between potential energy derived by pair potentials and calculations from EAM model may be attributed to the neglect of the electron background energy in pair potentials. The results also reveal that the uncertainty of experimental data affects greatly the accuracy of the pair potential.

DOI: 10.1103/PhysRevB.75.014106 PACS number(s): 34.20.Cf, 61.25.Mv

I. INTRODUCTION

Computer simulation studies, which can provide an atomistic understanding of structural and dynamic quantities in liquids or glasses, have been an important complementarity to experimental studies. The key quantity in the computer simulation is an assumed knowledge of the interatomic potential. Currently, several empirical[1,2] and theoretical methods[3,4] have been used to construct potentials for transition metals. One of the most popular potentials is the empirical determination of pair potential $\Phi(r)$, which expresses directly all equilibrium properties of liquids in conjunction with pair correlation function $g(r)$. Various model pair potentials such as the hard-sphere potential, inverse power potential, Lennard-Jones (LJ) potential, and effective ion-ion potential are frequently used in numerical calculations. In particular, the LJ potential, which can be considered as a simple empirical expression, has been widely used to model a wide range of materials, ranging from the rare gas solids to metallic liquids.[5–7] It is also the potential of choice in studies when the focus is on fundamental issues, rather than on properties of specific materials.

Of course, the interactions in real materials are more complex than that described by a simple pair interaction, especially in liquid metals where the pair potential requires far longer range oscillatory interactions resulting from the presence of conduction electrons.[8,9] In the past 20 years, it has been well accepted that many-body effects play an important role in the behavior of metals and alloys. The embedded atom method (EAM) proposed by Daw and Baskes[10,11] is one of the successful methods that combines the computational simplicity and the physical picture with many-body effects. In this approach, the dominant energy of the metal is viewed as the energy to embed an atom into the local electron density due to the remaining atoms of the system. However, in the determination of LJ or EAM potentials, model parameters are often chosen by fitting to reproduce one or more experimental information around the equilibrium solid, such as lattice parameter, elastic constants, vacancy-formation and migration energies, and cohesive energy of the lattice. Liquid-state calculations are then provided to test the functional form. Actually, the liquid data should be used to improve the choice of the potential forms.[12] Therefore, the major purpose of our work is to derive modified LJ potentials for liquid metals which properly take into account the experimental data of liquids.

The viscosity of liquid metals is one of important transport coefficients of fluids from the viewpoint of both practical production and investigations of the structure of liquid metals. Various empirical formulas, such as the well-known Arrhenius type, have been available for the viscosity of liquid metals over a wide range of temperatures. Recently, a dense gaslike model was proposed[13] to describe the viscosity for liquid metals by examining the Enskog formula of the viscosity for dense gases. One of adjustable parameters in the formula is the activation energy, which is roughly related to the maximum depth in the attractive part of the pair potential for liquid metals. So, as described below in the present paper, it is possible to speculate the pair potential of liquid metals by use of Born-Green (BG) formula of the viscosity with the experimental viscosity and pair correlation functions.

In this paper, we are trying to provide the pair potentials for fcc metals Cu and Ag which are based on the dense gaslike model of viscosity for liquid metals. Then we proceed to the application of these pair potentials to studies of energy and structural transition during rapid cooling by molecular dynamics (MD) simulations.

II. SIMULATION METHODS

A. The modified Lennard-Jones potential and the effective potential of the EAM

The LJ potential consists of the short-range repulsive part of the power $1/r^{12}$ and the long-range attractive part of the power $1/r^6$, where r is the distance between atoms or molecules. It is well known[14] that the long-range attractive part is due to the so-called van der Waals interactions arising

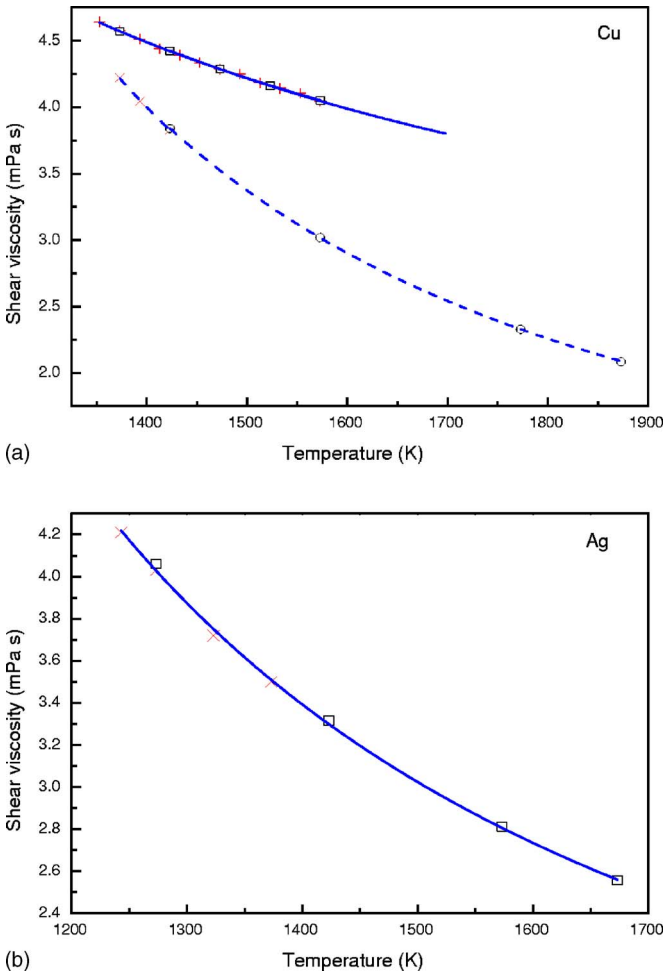

FIG. 1. (Color online) The viscosities of the liquid Cu and Ag. The solid and broken curves are the calculated results for each set of experimental data. The experimental data in Refs. 24 and 25 are denoted by the mark of (×) and (+), respectively; the calculated results used in the Born-Green formula Eq. (18) are indicated by the mark of (○) and (□).

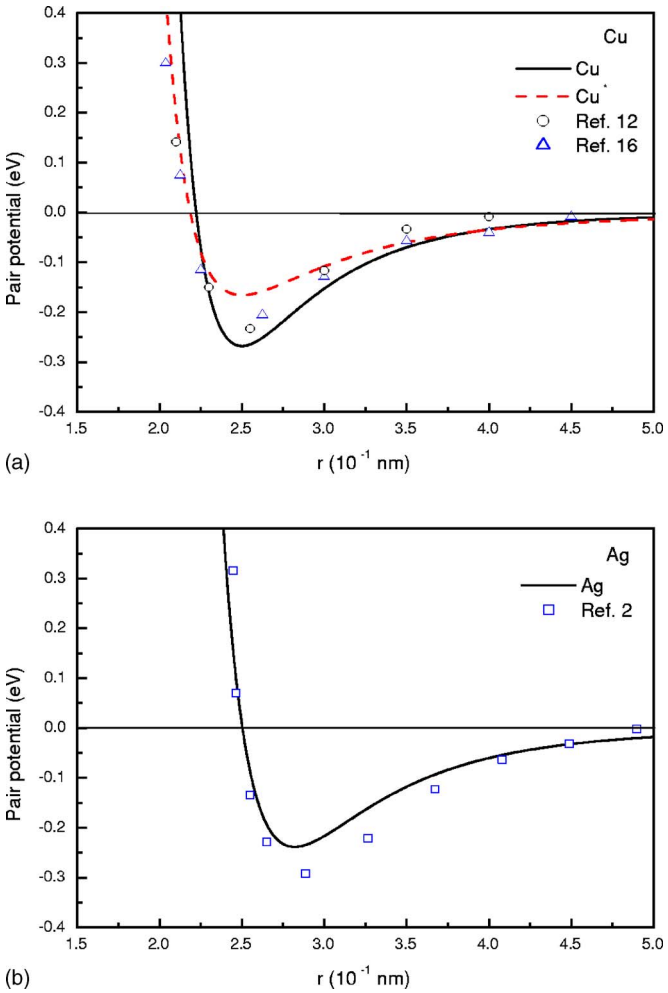

FIG. 2. (Color online) The pair potentials of the liquid Cu and Ag. The solid and broken curves in (a) are the obtained results Cu and Cu*, respectively. The squares, circles and triangles correspond to other theoretical potentials in Refs. 2, 12, and 16, respectively.

from the dipole moments of atoms; and the short-range repulsive part is due to the Pauli exclusion principle in the short-range regions where the orbital electrons of atoms or molecules overlap. The power $1/r^{12}$ is chosen for mathematical simplicity, but can fit well experimental data for gas phases and rare-gas liquids.

For a liquid metal, the long-range attractive part of the potential significantly differs from that of rare-gas liquids due to the conduction electrons, and the short-range repulsive part becomes slightly softer than that of the LJ potential.[15] In the present work, we shall modify the long-range attractive part, but, for simplicity, keep the power $1/r^{12}$ for the short-range repulsive part of the LJ potential as a first approximation. Our modified LJ potential is as follows:

$$\phi(r) = 4\varepsilon\left[\left(\frac{\sigma_0}{r}\right)^{12} - \left(\frac{\sigma_0}{r}\right)^{6-\theta}\right], \tag{1}$$

where ε, σ_0, θ are parameters, and the additional parameter θ is introduced to modify the long-range attractive part in the LJ potential. Thus, our modified LJ potential has three parameters $(\varepsilon, \sigma_0, \theta)$ which are related to the maximum depth E_m and its position r_m as

$$\sigma_0 = r_m\left(\frac{6-\theta}{12}\right)^{1/(6+\theta)}, \tag{2}$$

$$\varepsilon = -\frac{E_m}{4}\left[\left(\frac{\sigma_0}{r_m}\right)^{12} - \left(\frac{\sigma_0}{r_m}\right)^{6-\theta}\right]^{-1}, \tag{3}$$

so that the modified LJ potential can be obtained by determining three parameters (E_m, r_m, θ). In the next section, we will present a procedure to determine these parameters.

In the present work, we compare results obtained by our modified LJ potential with those by the embedded atom method (EAM) that assumes the total energy E of a system with N atoms as

$$E = \sum_i F_i(\rho_i) + \frac{1}{2}\sum_{\substack{i,j \\ (i\neq j)}} \phi_{ij}(r_{ij}), \tag{4}$$

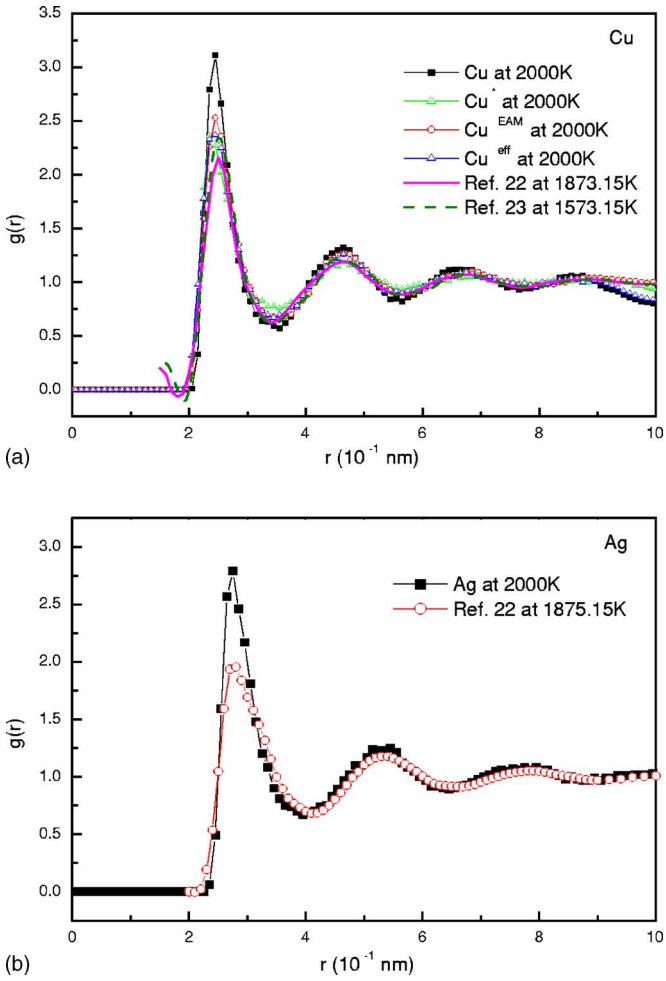

FIG. 3. (Color online) The calculated and experimental pair correlation functions of liquid Cu and Ag.

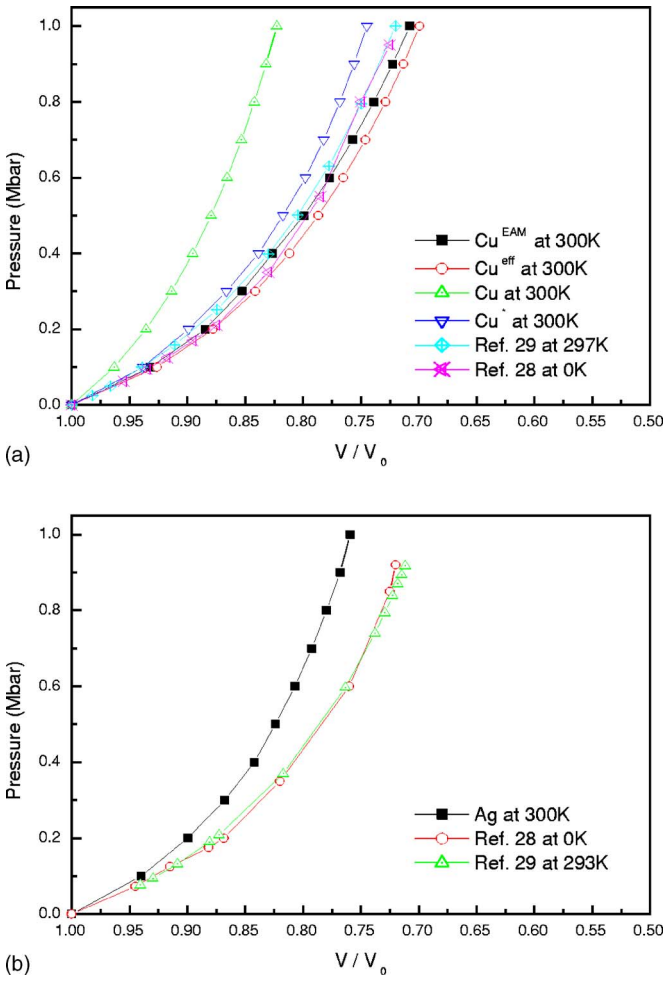

FIG. 4. (Color online) The calculated and referenced equation of states at 300 K for Cu and Ag.

$$\rho_i = \sum_{j(\neq i)} f_j(r_{ij}), \tag{5}$$

where ρ_i is the electron density at atom i due to the rest of atoms, f_j is the electron density of atom j as a function of distance from its center, F_i is the energy to embed an atom in an electron density ρ_i, and $\Phi_{ij}(r_{ij})$ is a two-body central potential between atoms i and j with the separation distance r_{ij}.

Following Foiles'[12] procedure for obtaining an effective potential, the total energy given by Eq. (4) is approximately decomposed into structure-independent and -dependent energies by a Taylor expansion around an average electron density $\bar{\rho}$ as

$$E = NE(\bar{\rho}) + \frac{1}{2}\sum_{i\neq j} \psi_{ij}^{eff}(r_{ij}), \tag{6}$$

with

$$E(\bar{\rho}) = F(\bar{\rho}) - \bar{\rho}F'(\bar{\rho}) \tag{7}$$

and

$$\psi^{eff}(r) = \phi_{ij}(r_{ij}) + 2F'(\bar{\rho})\rho(r) + F''(\bar{\rho})[\rho(r)]^2, \tag{8}$$

where $F'(\bar{\rho})$ and $F''(\bar{\rho})$ denote the first two derivatives of the embedding energy at $\bar{\rho}$. The structure-dependent term $\psi^{\text{eff}}(r)$, defined by Eq. (8) is called the effective potential,[12] and hence we call the structure-independent term $E(\bar{\rho})$, defined by Eq. (7) as the electron background energy.

By replacing atomic electron density with an exponentially decaying function, Johnson[16] developed a set of simplified EAM functions for fcc metals. The electronic density in his model is taken as

$$f(r) = f_e \exp\left[-\beta\left(\frac{r_1}{r_{1e}} - 1\right)\right], \quad r \leqslant r_c, \tag{9}$$

and the two-body potential is taken as a Born-Mayer repulsion with the same analytic form as $f(r)$,

$$\phi(r) = \phi_e \exp\left[-\gamma\left(\frac{r_1}{r_{1e}} - 1\right)\right], \quad r \leqslant r_c, \tag{10}$$

where r_c is a cutoff parameter, β and γ are model parameters, and the subscript e is used to indicate evaluation at equilibrium.

It was pointed out by Daw and Baskes[11] that, for the case in which the embedding function is linear in ρ, the entire scheme is equivalent to using a different pair potential. Ignoring the third term in Eq. (8), the effective pair potential reduces to[16]

$$\psi^{eff}(r) = \phi_e \left[e^{-\gamma(r/r_{1e}-1)} - \frac{\gamma}{\beta} e^{-\beta(r/r_{1e}-1)} \right], \tag{11}$$

$$\phi_e = \frac{5G_e\Omega_e}{2\gamma(\gamma-\beta)}, \tag{12}$$

where G is the average shear constant and Ω is the atomic volume. Details of the formulas are given in Ref. 16.

The effective potential $\psi^{\text{eff}}(r)$ defined by Eq. (11) should be compared with our modified LJ potential $\Phi(r)$ given by Eq. (1). The energies for the EAM that we will calculate in Sec. III are the total energies given by Eq. (4), whereas those for the effective potential and the modified LJ potential are the energies without the electron background energy.

B. The dense gaslike model and the Born-Green formula

We follow Morioka's procedure[13] for determining the parameters in the modified LJ potential presented in the previous section. In this procedure, two kinds of formulas of viscosity for liquids are employed. This is briefly described below.

In order to construct a more advanced model derived in a more general kinetic theory rather than a simple equilibrium kinetic theory, a formula of the viscosity for dense gases of the hard-sphere fluids firstly derived by Enskog[17] is referred, which is written as

$$\eta = \eta_g \left[\frac{1}{g(\sigma)} + 0.8nb + 0.761(nb)^2 g(\sigma) \right], \tag{13}$$

with

$$b = \frac{2\pi}{3}\sigma^3, \tag{14}$$

where n is the number density, σ is the diameter of the hard-sphere fluids, $g(\sigma)$ is the value of the pair correlation function (PCF) at the surface of the hard-sphere fluids, and η_g is the viscosity in the gas phase,

$$\eta_g = \frac{5}{16N_A\sigma^2}\sqrt{\frac{MRT}{\pi}}, \tag{15}$$

where N_A is Avogadro's number, M is the mass of the atom, R is the gas constant, and T is the absolute temperature. The Enskog formula (13), as it stands, is not able to describe correctly the observed temperature dependence of viscosity for dense fluids such as liquids. The purpose to introduce the dense gaslike model[13] is to remedy this defect by considering physical characters of the pair potential and PCF. In the result,[13] $g(\sigma)$ is speculated as

$$g(\sigma) \to \exp\left(\frac{E}{RT}\right), \tag{16}$$

where E is the activation energy that relates to the potential of mean force acting on the atom around the position of the maximum depth of the pair potential.

Substituting Eq. (16) into Eq. (13), one obtains a modified Enskog formula in which the last term dominates over the first two terms in the low temperature regions. The formula may be approximated by

$$\eta \cong 0.761b^2n^2\eta_g \exp\left(\frac{E}{RT}\right). \tag{17}$$

Values for E and σ in the above formula are determined by fitting to the experimental viscosities extending to a wide range of temperature. This is what we call the dense gaslike model. It is clear that the formula of viscosity given by Eq. (17) is able to describe correctly the temperature dependence due to the form of the Arrhenius type.

By examining various kinds of liquid metals, the work[18] found that σ approximately equals to r_m^{exp}, the position of the experimental first peak of PCF, and that E of Cu and Ag to the maximum depth E_m in the empirical pair potentials, i.e. $E \sim E_m$. In this way, the dense gaslike model roughly determines E_m.

In order to determine the other two parameters (r_m, θ), we shall employ the Born-Green (BG) formula of viscosity for liquids,[19]

$$\eta = f_{\text{BG}}\frac{2\pi}{15}\left(\frac{M}{RT}\right)^{1/2}\frac{n^2}{N_A}\int_0^\infty g(r)\frac{d\phi(r)}{dr}r^4 dr, \tag{18}$$

where f_{BG} is an additional parameter arising from an incomplete formulation of Born and Green.[20,21] Nevertheless, we employ the BG formula due to the following reason: In the limit of hard-sphere liquids, the BG formula reduces to the last term in the Enskog formula (13) on which the dense gaslike model is based, with a constant factor. Therefore, the BG formula may be regarded as a simply generalized Enskog formula extended to a realistic dense fluid, so that we expect that, by employing the BG formula, the parameters (E_m, r_m, θ) in our modified LJ potential can be determined consistently with the result of the dense gaslike model, although the BG formula has the additional parameter f_{BG}.

In order to calculate the BG formula, one needs to know $g(r)$ beforehand. Hence, we start with the experimental PCF,[22,23] using the experimental data of r_m^{exp} for r_m in our potential, since the position of the first peak of PCF is close to the position of the maximum depth of the potential. Employing the BG formula, the last parameter θ is thus determined by fitting to the experimental viscosities.[24,25]

Thereafter, the potentials derived by the experimental viscosities[24] and $g(r)$ (Ref. 22) will be called the case Cu (Ag), while that calculated from the experimental data in Refs. 25 and 23 will be marked as Cu*.

C. Details of MD simulations

The MD simulations were performed using a system with 500 atoms in a cubic box under periodic boundary condi-

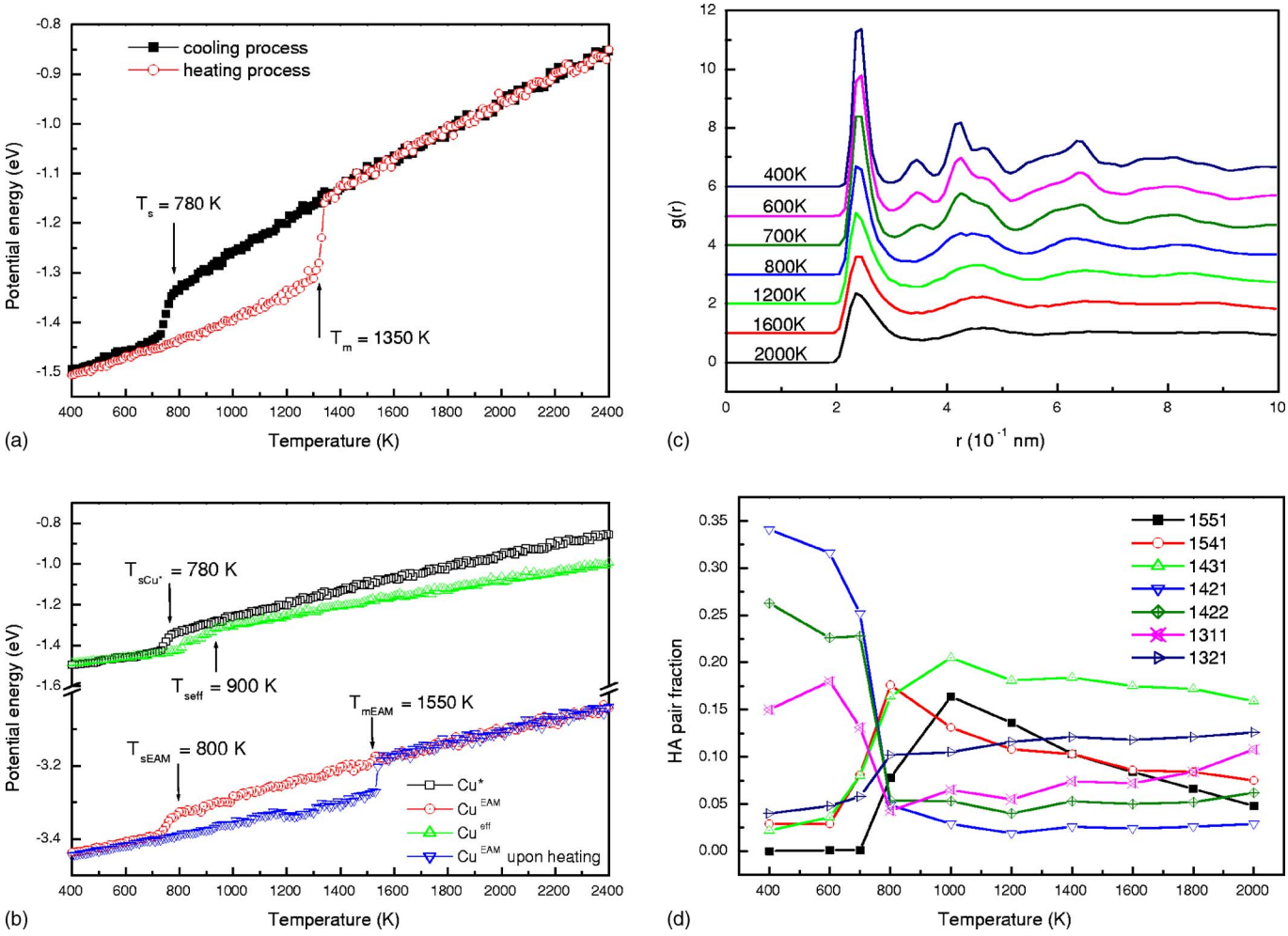

FIG. 5. (Color online) The energy and structural transitions of liquid Cu*. (a) potential energies for heating and cooling cycles; (b) results of potential energy derived by the current pair potential (squares), Johnson's EAM model (circles) and effective pair potential (triangles), respectively; (c) PCF; (d) variation of the fractions of HA indices.

tions. The temperature was kept constant by the Nose-Hoover thermostat method and the equations of motion were integrated using the Verlet velocity algorithm. To maintain the stability of the algorithm, the time step was chosen to be 3.5 fs and 1.28 fs, respectively, in simulations of Cu and Ag.

We equilibrated the system for 100 000 time steps in a constant temperature and constant pressure (NPT) condition at $T=2400$ K. This was followed by a cooling process in which the liquid Cu (Ag) was cooled from 2400 K to 400 K with a cooling rate of 2.86 K ps^{-1} (7.8 K ps^{-1}). At selected temperatures, the velocities and the positions of atoms were noted every 100 time steps.

III. NUMERICAL RESULTS AND DISCUSSIONS

Following the procedure presented in the previous section, we examined two kinds of transit liquid metals of Cu and Ag. In the calculations for viscosities, we need to know the number density n in Eqs. (17) and (18). The number density is related to the atomic density ρ as

$$n = \frac{\rho}{M} N_{\mathrm{A}}, \tag{19}$$

and hence we used an empirical formula for ρ given in Ref. 26,

$$\rho = \rho_m + \Lambda(T - T_m), \tag{20}$$

where ρ_m is the density at the melting point T_m, and Λ is a parameter. The values for ρ_m, T_m, and Λ in our calculations, as well as other input parameters, are listed in Table I.

The model parameters obtained for each set of experimental data are also listed in Table I. Here, in addition to fitting the experimental viscosities, we have made adjustments for the value of E, to obtain a more satisfactory accuracy of our potentials and simulations in the following applications, namely, in the calculations of PCF, EOS, potential energy versus temperature, and structural transition in the cooling process. Hence, our obtained parameters slightly differ from those given in Ref. 13. The results in Table I reveal that the values of σ are slightly smaller or higher than the observed atomic diameter d. Since the values of d are close to the

experimental r_m, which may be regarded as the average atomic diameter in liquids, it is reasonable to conclude that the calculated σ is comparable with the actual atomic diameter in liquid metals.

Figure 1 presents the calculated viscosities of Cu and Ag by the model formula (17) and the Born-Green formula (18), showing that these results are in good agreements with the experimental viscosities in a wide range of temperatures. Moreover, we can see that the temperature dependence of the two formulas is in accordance with the Arrhenius type. It is notable from Fig. 1(a) that the experimental viscosities of Ref. 25 are clearly higher than those in Ref. 24, causing differences in the two sets of model parameters listed in Table I. So far it is very difficult to state definitely the accuracy of viscosity measurements for liquid metals. Errors of ±1% to ±20% would seem to be a fair estimate with the exception of a few metals.[26] Therefore, an involved problem in the application of the dense gaslike model is which set of experimental viscosities is more appropriate for the subsequent construction of pair potential for liquid metals.

A comparison between pair potentials for Cu and Ag based on the dense gaslike model and other theoretical potentials[2,12,16] derived from an analysis for solid characters is given in Fig. 2. Qualitatively, these potentials are similar with the comparable value and position of the maximum depth; however, the current potentials are simply longer ranged without a long-range repulsive barrier. In the cases of Cu^*, despite a small value for E in the potential, the value of θ in this potential is much larger than that in the potential of Cu, leading a longer ranged attractive part of pair potential. Additionally, the repulsive term of the potentials Cu^* and Ag are both consistent with other theoretical potentials,[2,12,16] while that of Cu is relatively "harder." Therefore, it is speculated that the affection from the attractive part to the repulsive term in the pair potential is not only due to the value of the modification parameter θ but also due to that of E. Incidentally, the inclusion of average effects of many-body terms will make the potentials softer than ours.

Figure 3 shows results of the calculated PCF for Cu and Ag, compared with the available experimental data in Refs. 22 and 23. In general, there is a good agreement between calculated and experimental results. At a more detailed level, however, we find that there are obvious variations in the heights of the successive maxima for different sets, although the positions remain almost unchanged. The calculations for Cu tend to overestimate the height of peaks in PCF, and the ascending process before reaching the first peak of $g(r)$ is relatively abrupt because of the "harder" pair potential as mentioned above. Contrastively, the shape of $g(r)$ calculated by the potential Cu^* shows a good agreement in the position and height of the first peak, but it appears slightly flat when the r is beyond the first neighbor distance. Since the height and position of the peak in PCF is the result of a delicate balance between the repulsive and attractive contributions to pair potentials,[27] these differences may be due to either the feature of pair potential or experimental errors or to the combined effects of both. MD simulations based on Johnson's EAM and effective pair potential show that the calculated $g(r)$ also overestimates the height of the first peak, as shown in Fig. 3(a). Additionally, analyses in PCF results of the two

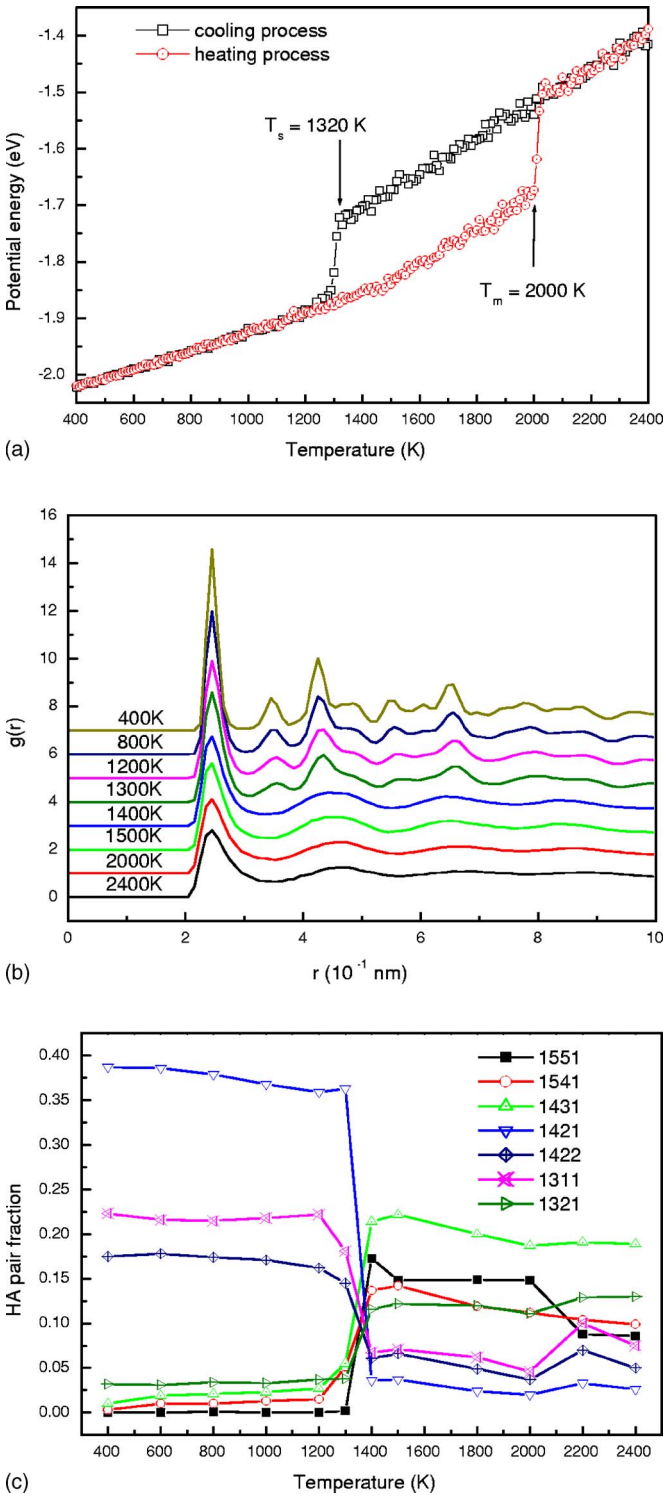

FIG. 6. (Color online) The energy and structural simulations of liquid Cu upon cooling. (a) Potential energies for heating and cooling cycles; (b) PCF; (c) variation of the fractions of HA indices.

cases of Cu reveal that the slower the descending of viscosity curve, the smaller the value of E, indicating a falling energy barrier for the movement of atoms in liquids, and consequently, the obtained PCF is much flatter. This suggests that the differences between the calculated and experimental PCF

TABLE I. The input parameters M, r_m, T_m, ρ_m, and $-\Lambda$, and the model parameters E, σ, f_{BG}, and θ. The ρ_m is in 10^3 kg m^{-3}, and $-\Lambda$ is in 10^1 kg m^{-3} K^{-1}.

	Inputs					Model parameters			
Metal	M (g/mol)	r_m (Å)	T_m (K)	ρ_m	$-\Lambda$	E (eV)	Σ (Å)	f_{BG}	θ
Cu	63.54	2.50	1356.15	8.00	8.0	0.268	2.01	1.355	0.255
Cu*						0.166*	3.11*	0.105*	1.919*
Ag	107.87	2.82	1233.65	9.33	9.1	0.238	2.68	1.196	0.406

are the results of experimental uncertainty as well as the limitations of pair potentials.

As we know that many aspects of the energetics of metals can be understood if the equation of state (EOS) is known. Here, we calculate the volume for solids Cu and Ag under different external pressures up to the pressure of 1 Mbar at 300 K. As shown in Fig. 4, the pressure-volume curves reproduced by present modified LJ potentials for Cu, Cu*, and Ag are compared with the theoretical results[28] and experimental data.[29] There are generally comparable results between the simulated EOS and other results, indicating that our modified LJ potentials display reasonable lattice dynamics behaviors. The poorer agreement for Cu may be associated with the obtained potential for Cu, which also makes a larger height of the first peak for PCF in liquid state as shown in Fig. 3(a).

Now let us apply the current potentials to study of rapid cooling processes via MD simulations. Due to the finite size of our system, a single melting temperature cannot be found in a straightforward manner. In this work, we first decrease the temperature of the liquid towards solidification and then raise the temperature of the solid to obtain the melting temperature, following Sadigh and Grimvall's procedure.[30] Figure 5(a) shows the potential energy of Cu* in cooling and heating cycles, indicating the melting temperature T_m=1350 K at the heating rate of 2.86 K ps^{-1}. It is comparable with the experimental melting point of 1356.15 K for pure Cu,[26] but is 200 K lower than the calculated result based on the EAM. Figure 6(a) indicates the melting point for Cu is 2000 K and the calculated heating curve for Ag plotted in Fig. 7(a) begins to deviate from linearity at 1940 K, both of which exhibit a high superheating temperature due to the high heating rate.

In this work we are mainly interested in the liquid phase of copper. Figures 5–7 show the potential energy and structural transitions in the cooling process for the cases of Cu*, Cu, and Ag, respectively. It can be seen from Fig. 5(b) that the potential energy of the case Cu* decreases with decreasing temperature and a sudden drop in energy arises at the solidification temperature T_s, demonstrating that the final system is a crystalline state. However, Fig. 5(b) reveals that although there are similar solidification temperatures, the value of the current potential energy is higher than that calculated by EAM model. To clarify this point, the temperature dependence of potential energy is studied with the effective pair potential given by the formula (11). The curve for potential energy [Fig. 5(b) marked by triangles] follows the trends for EAM model reasonably well, while the value of potential energy, which is comparable with the results calculated by our current potential, is evidently higher than the energy value for EAM model. We have analyzed the calculation procedure of the energy in the Sec. II A, and suggested that the differences in values of energy may be attributed to the neglect of the electron background energy.

The final state of the system can also be verified conveniently in terms of the results of PCF shown in Fig. 5(c). Clearly, the PCF retains a characteristic of liquid phase as the temperature is higher than 800 K; in contrast, crystal peaks can be detected at 700 K and become more obvious with the decreasing temperature. More detailed information on the microstructure of the system as a function of temperature can be obtained by Honeycutt-Anderson (HA) (Ref. 31) analysis. Figure 5(d) shows that there is a linear increase in three types of pairs, 1551, 1541, and 1431 bonded pairs, as the temperature decreases to 800 K; while other pairs, such as 1421, 1422, 1311, and 1321 bonded pairs remain nearly a constant. A further decrease of temperature leads to a significant change in these bonded pairs. For example, the numbers of 1551, 1541, 1431, and 1321 bonded pairs drop to nearly zero at a low temperature of 400 K. On the contrary, the number of 1421 bonded pair shows a sharp increase to 34.1% at 400 K; 1422 and 1311 bonded pairs also increase obviously, implying a crystallized sample that consists of both fcc struc-

TABLE II. Main structural parameters for different systems at the temperature of 400 K. Cu^{EAM} and Cu^{eff} are the cases calculated via MD simulations based on Johnson's EAM and effective two-body potential, respectively. Parameters for fcc are obtained from Ref. 31.

	Cu	Cu*	Cu^{EAM}	Cu^{eff}	Ag	fcc
Q_6	0.52301	0.50605	0.49524	0. 47280	0.57217	0.574148
W_6	−0.02131	−0.0162	−0.01418	−0.01703	−0.01732	−0.013161
CN	9.3276	9.604	9.7096	8.7404	9.5884	12

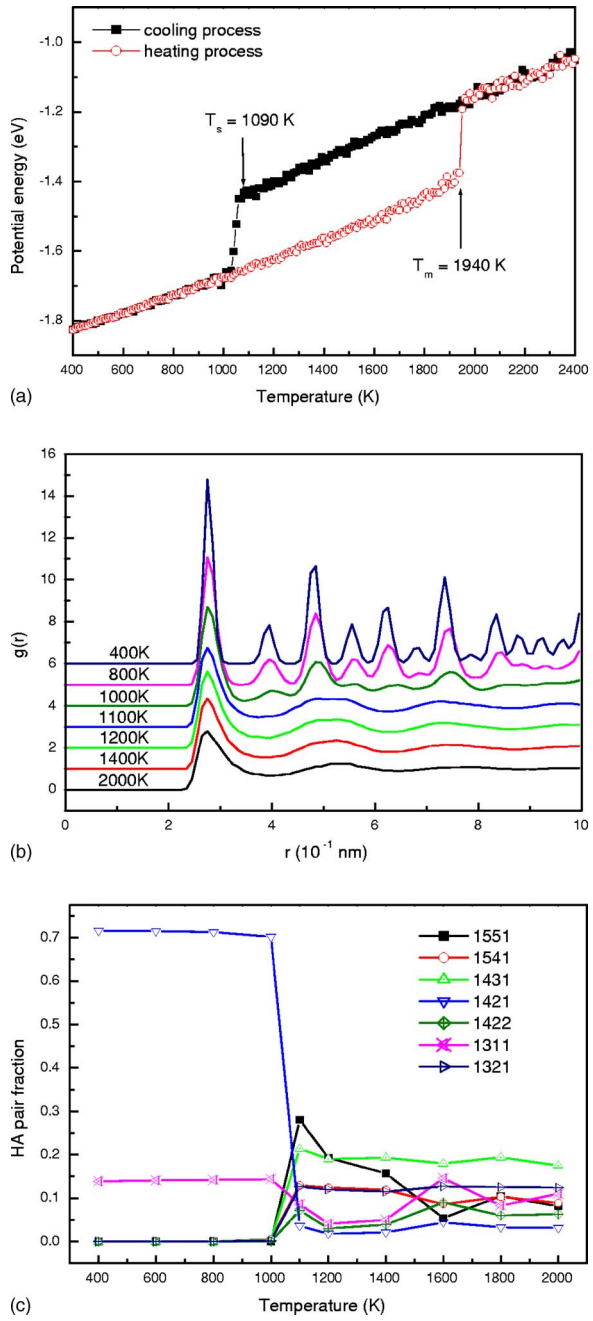

FIG. 7. (Color online) The temperature dependence of energy and structure in liquid Ag in the process of cooling. (a) Potential energies for heating and cooling cycles; (b) PCF; (c) variation of the fractions of HA indices.

ture and a spot of hcp and rhombohedral order. Additionally, it can be seen from Table II that for the case of Cu*, the bond orientational order parameter[32–34] W_6 at 400 K is −0.0162, which is slightly lower than the value of −0.013161, indicative of an ideal fcc order. We are also delighted to find similar variations in potential energy and structure for the cases of Cu and Ag, except that the final sample of Ag only consists of 1421 and 1311 bonded pairs. Moreover, the calculated structural parameters listed in Table II are comparable with results from other potentials and experiments, so it is reasonable to conclude that the current pair potential can describe well the solidification of liquid metals.

It is also notable that just before the crystallization temperature, there are numerous 1551, 1541, and 1431 bonded pairs characterizing the liquid and glassy structure, which implies an increasing disorder in the microstructure of system. Classical nucleation theory (CNT) assumes that crystallization occurs via a process of nucleation at random sites, after an undercooling dependent delay time, followed by crystal growth.[35] Only after an incubation regime with high free energy through atomic fluctuation can the system enter the steady stage of nucleation and crystallization. Therefore, we deduce that the increasing disorder in the simulated sample characterizes the process of atomic fluctuation when clusters with overcritical size may grow continuously while undercritical-sized crystallites tend to dissolve, in both cases, to lower their free energy.[36]

IV. CONCLUSION

In this paper, we have constructed the modified Lennard-Jones potentials of liquid Cu and Ag using the dense gaslike model and Born-Green formula of viscosity for liquid metals. In contrast with other potentials parameterized by solid-state data, the present process for constructing our potentials involve the liquid density, experimental viscosity, and PCF, and therefore, the obtained modified LJ potentials are in accordance with characteristics of liquid metals. However, the uncertainty of experimental data has an unavoidable influence on the calculated pair potential.

MD simulations based on the current pair potentials have lead the results of EOS for solids Cu and Ag at 300 K, which indicates that the modified LJ potentials display reasonable lattice dynamics behaviors. The calculated PCF for liquids at 2000 K are comparable to the experimental data and the difference in the height of peaks results from both the pair potential and experimental uncertainty. Results of MD simulations upon cooling reveal that the modified LJ potential can provide an accurate reproduction for the liquid-solid phase transition and a fcc crystalline state is distinctly detected at low temperatures. The neglect of the electron background energy results in the differences in potential energy derived by pair potentials and calculations from Johnson's EAM model.

Analyses of the results of HA pairs reveal that a disordered microstructure appearing before the crystallization represents a characteristic process of atomic fluctuation in liquids which is necessary to the successive nucleation and crystallization.

ACKNOWLEDGMENTS

The authors are grateful for the support of the National Natural Science Foundation of China (Grant No. 50501012 and No. 50301008) and the Natural Science Foundation of Shandong Province (No. 2004BS04016). We appreciate T. Mao and S. J. Cheng for their valuable experimental data. We are also grateful to Shandong High Performance Computing Center for fruitful computations.

*Corresponding author. Email address: wanglihxf@sdu.edu.cn

[1] R. A. Johnson, J. Phys. F: Met. Phys. **3**, 295 (1973).
[2] M. I. Baskes and C. F. Melius, Phys. Rev. B **20**, 3197 (1979).
[3] M. Rasolt and R. Taylor, Phys. Rev. B **11**, 2717 (1975).
[4] A. E. Carlsson, M. L. Klein, and H. Ehrenreich, Philos. Mag. A **41**, 241 (1980).
[5] W. C. Swope and H. C. Andersen, Phys. Rev. B **41**, 7042 (1990).
[6] J. Q. Broughton and G. H. Gilmer, J. Chem. Phys. **79**, 5095 (1983).
[7] E. J. Jensen, W. D. Kristensen, and R. M. J. Cotterill, Philos. Mag. **27**, 623 (1973).
[8] J. Friedel, Philos. Mag. **43**, 153 (1952).
[9] W. A. Harrison, *Pseudopotentials in the Theory of Metals* (Benjamin, New York, 1966).
[10] M. S. Daw and M. I. Baskes, Phys. Rev. Lett. **50**, 1285 (1983).
[11] M. S. Daw and M. I. Baskes, Phys. Rev. B **29**, 6443 (1984).
[12] S. M. Foiles, Phys. Rev. B **32**, 3409 (1985).
[13] S. Morioka, J. Non-Cryst. Solids **341**, 46 (2004).
[14] C. Kittel, *Introduction to Solid State Physics* (John Wiley, New York, 1986).
[15] J. P. Hansen and I. R. McDonald, *Theory of Simple Liquids* (Academic Press, New York, 1986).
[16] R. A. Johnson, Phys. Rev. B **37**, 3924 (1988).
[17] S. Chapman and T. G. Cowling, *The Mathematical Theory of Non-uniform Gases* (Cambridge University, London, 1952).
[18] S. Morioka, X. F. Bian, and M. H. Sun, Z. Metallkd. **93**, 288 (2002).
[19] M. Born and H. S. Green, Proc. Roy. Soc. London **A190**, 455 (1947).
[20] M. Shimoji, Adv. Phys. **16**, 705 (1967).
[21] S. Morioka, Phys. Rev. E **72**, 051203 (2005).
[22] Y. Waseda, *The Structure of Non-Crystalline Materials* (McGraw-Hill, New York, 1981).
[23] S. J. Cheng, PhD thesis, Shandong University, 2004.
[24] T. Iida, Z. Morita, and S. Takeuchi, J. Jpn. Inst. Met. **29**, 1169 (1975).
[25] T. Mao, X. F. Bian, X. Y. Xue, Y. N. Zhang, J. Guo, and B. A. Sun, Physica B **387**, 1 (2007).
[26] T. Iida and R. I. L. Guthrie, *The Physical Properties of Liquid Metals* (Oxford University, Oxford, 1988).
[27] G. M. Bhuiyan, M. Silbert, and M. J. Stott, Phys. Rev. B **53**, 636 (1996).
[28] J. H. Rose, J. R. Smith, F. Guinea, and J. Ferrante, Phys. Rev. B **29**, 2963 (1984).
[29] H. K. Mao, P. M. Bell, J. W. Shaver, and D. J. Steinberg, J. Appl. Phys. **49**, 3276 (1978).
[30] B. Sadigh and G. Grimvall, Phys. Rev. B **54**, 15742 (1996).
[31] J. D. Honeycutt and H. C. Anderson, J. Phys. Chem. **91**, 4950 (1987).
[32] D. R. Nelson and J. Toner, Phys. Rev. B **24**, 363 (1981).
[33] P. J. Steinhardt, D. R. Nelson, and M. Ronchetti, Phys. Rev. Lett. **47**, 1297 (1981).
[34] P. J. Steinhardt, D. R. Nelson, and M. Ronchetti, Phys. Rev. B **28**, 784 (1983).
[35] H. J. Schöpe, G. Bryant, and W. vanMegen, Phys. Rev. Lett. **96**, 175701 (2006).
[36] P. Beaucage and N. Mousseau, Phys. Rev. B **71**, 094102 (2005).